



Magnetically separable ZnFe₂O₄ nanoparticles: A low cost and sustainable catalyst for propargyl amine and NH-triazole synthesis

Roktopol Hazarika^a, Anirban Garg^a, Swadhin Chetia^a, Parmita Phukan^a, Akshay Kulshrestha^b, Arvind Kumar^b, Ankur Bordoloi^c, Amlan Jyoti Kalita^d, Ankur Kanti Guha^d, Diganta Sarma^{a,*}

^a Department of Chemistry, Dibrugarh University, Dibrugarh 786004, Assam, India

^b AcSIR, Salt and Marine Chemicals Division, CSIR-Central Salt and Marine Chemicals Research Institute, Bhavnagar 364002, India

^c Nano Catalysis, Catalytic Conversion and Process Division, CSIR -Indian Institute of Petroleum, Mohkampur, Dehradun 248005, India

^d Department of Chemistry, Cotton University, Panbazar, Guwahati, Assam, 781001

ARTICLE INFO

Keywords:

A³-coupling
Multicomponent reaction
Magnetically separable catalyst
Propargyl amine
NH-triazole
Computational study

ABSTRACT

The multicomponent reaction (MCR) strategy for the construction of important molecular scaffolds is in trending nowadays and among them, A³-coupling stands in a significant position. Aldehyde, amine and alkynes are coupled in this particular reaction via C-H activation process. Herein, we have reported zinc ferrite nanoparticles as magnetically separable heterogeneous catalyst for A³-coupling reaction with attractive attributes like excellent productivity, selectivity and better reusability. Moreover, the catalyst can also be effectively applied for the synthesis of various NH-triazoles with quantitative yields of the products. A plausible mechanism has been proposed for the synthesis of NH-triazoles followed by validation with computational study.

1. Introduction

Designing novel reaction strategies with high yield and negligible by-product formation are of great importance in this present era from the environmental as well as physiological point of view. MCRs stand high as one of the principal tactics in this aspect as these reaction strategies are atom economic in nature and very much strict in by-product formation that significantly contributes towards “Green Chemistry”. The MCR technique emerges as a powerful tool to build up a library of structurally complexed molecules with diverse elements in a single synthetic step [1]. Recently, such strategies have been widely applied in numerous organic transformations such as triazole formation, propargyl amine formation etc. The MCR strategy for propargyl amine synthesis consists of coupling of aldehyde, alkyne and amine respectively and is commonly accepted as A³-coupling reaction. Classically, the propargylamine derivatives have been synthesized via nucleophilic addition of Grignard reagents with enamines or by addition of lithium acetylides with imines [2]. However, the multistep preparative methods and storage issue due to sensitivity towards moisture or water make these reagents inappropriate for organic transformations. As an alternative, low cost, nontoxic transition metal catalysts have been employed for the construction of the propargyl amine derivatives via C-H activation

process [3]. Gholinejad et al. reported several gold and copper catalyzed A³ coupling reactions [4]. Propargyl amines are very interesting molecular entities which open up new ways to access versatile synthetic molecular scaffolds. Propargyl amines serve as intermediate to the synthesis of many biologically active compounds as well as natural products such as β-lactams, herbicides, fungicides etc. [5]. Moreover, some of them have been tested and approved as drug molecules against neurological diseases in the likes of Parkinson's and Alzheimer's diseases [6,7].

Literature indicates that a good number of reports are available regarding the synthesis of propargyl amine which are predominantly based on copper and silver [8]. However, adverse cytotoxicity effect or the high cost of these coinage metals demand replacement with inexpensive yet efficient metal catalyst. In this context, Zn is considered as a suitable alternative with very few examples citing its use in catalysis [9]. Therefore, Zn is chosen as the first preference for the aforesaid reaction.

In recent years, magnetic nanoparticles (MNPs) have established themselves as a material of prodigious significance in different fields especially in ferrofluids, magnetic drug transportation, magnetic data storage devices, magnetic separations, magnetic resonance imaging (MRI) and magnetic fluid hyperthermia treatment for malicious growth [10]. Moreover, applying MNPs as catalyst can afford simple separation

* Corresponding author.

E-mail addresses: dsarma22@gmail.com, dsarma22@dibru.ac.in (D. Sarma).

<https://doi.org/10.1016/j.apcata.2021.118338>

Received 26 July 2021; Received in revised form 25 August 2021; Accepted 25 August 2021

Available online 1 September 2021

0926-860X/© 2021 Elsevier B.V. All rights reserved.

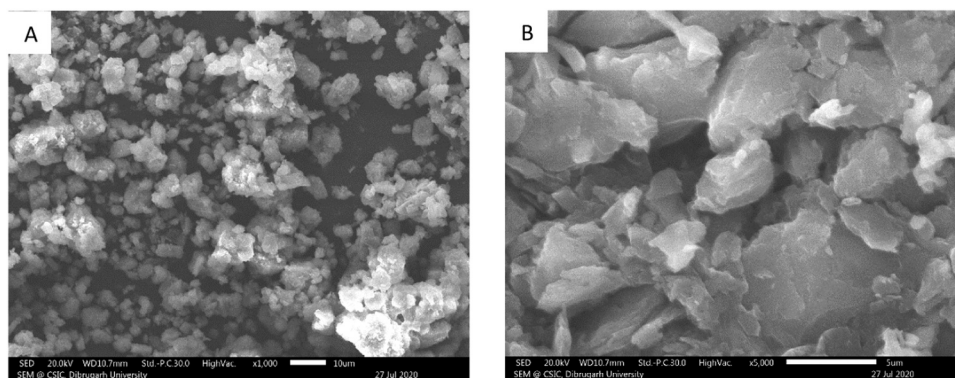


Fig. 1. (A) and (B): SEM images for the zinc ferrite nanoparticles.

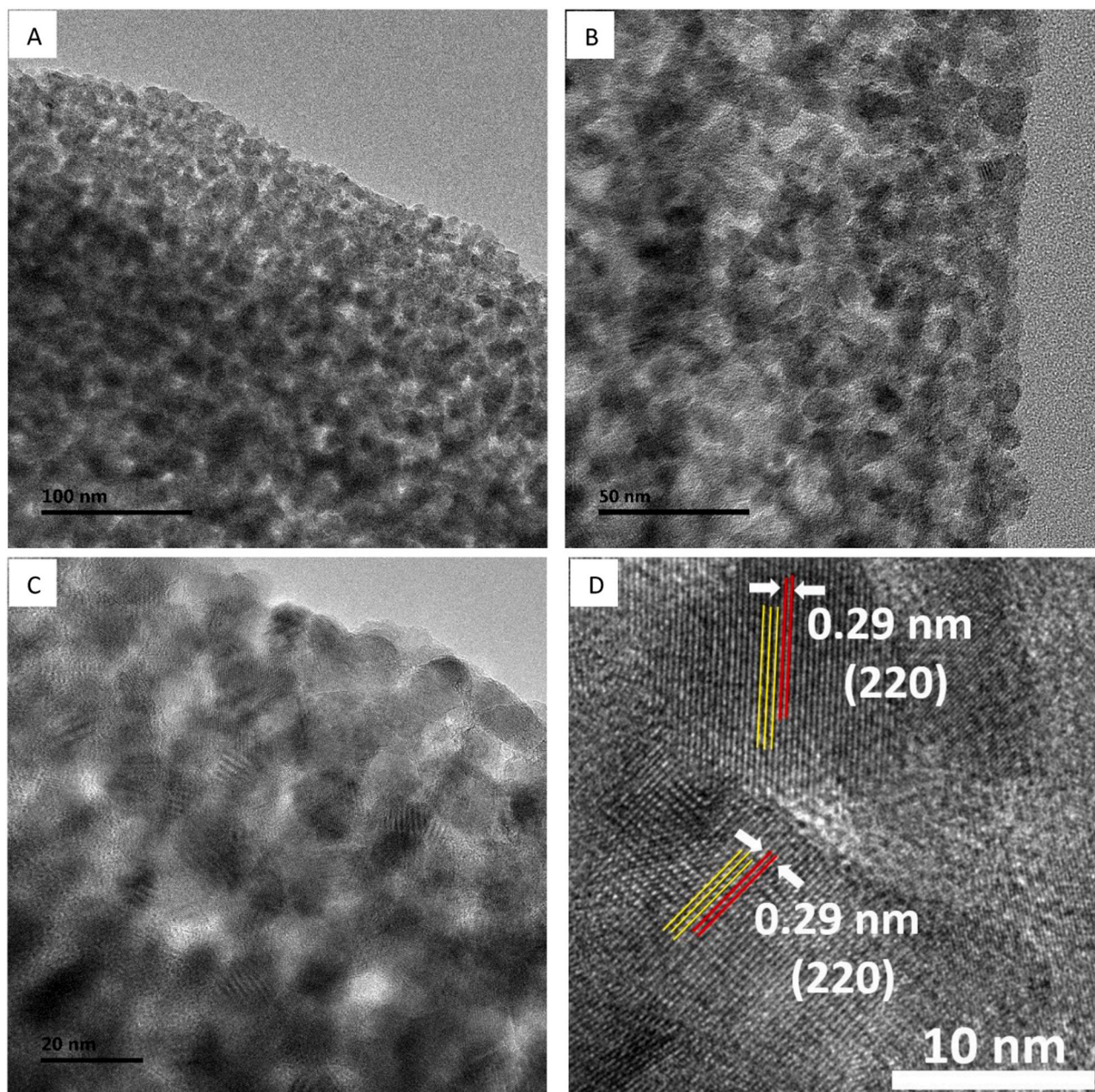


Fig. 2. TEM (a and b) and HRTEM (c and d) images for ZnFe₂O₄.

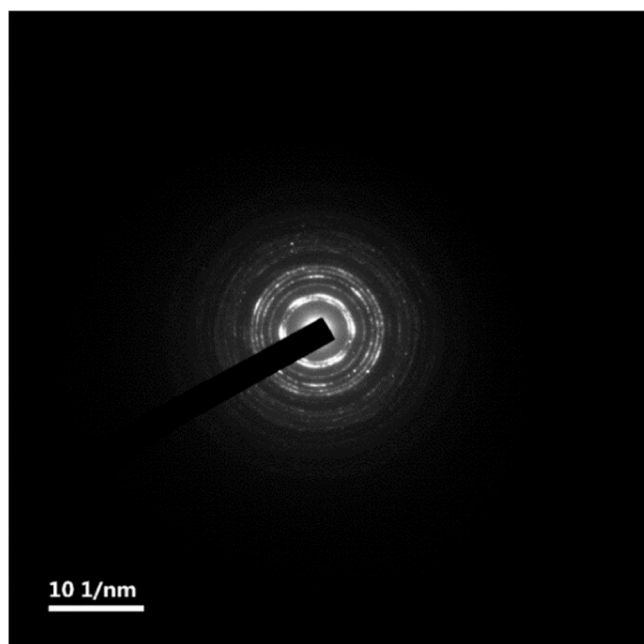


Fig. 3. SAED pattern of ZnFe₂O₄.

of the catalyst from the reaction mixture by the application of an external magnet genuinely enhancing reusability with minimal loss in the catalyst loading. In this regards, spinel compounds especially ferrite system plays vital role. Different ferrite systems based on transition metals as well as different metal organic frameworks were successfully applied in various organic reactions [11]. Facile synthetic procedures, inexpensive nature, economic efficiency, availability of high percentage of surface area, insolubility in reaction media, easy recovery and superior catalytic activity make these mixed metal oxide nanoparticles (MMONs) more advantageous to the individual component oxides in diverse catalysis [12].

Owing to these attractive characteristics, magnetically separable catalysts are very much trending in modern applications. Therefore, we thought of applying such catalytic system for our desired transformations.

In recent years, literature reveals that ZnFe₂O₄ nanoparticles have been efficaciously screened in various catalytic transformations into pyrano pyrimidines [12], isatinyldenethiazol-4-one [13], 1,4-dihydropyridines [14], 2-amino-3-cyano-4H-pyran [15] etc. as these nanoparticles are inexpensive, very much effective with high catalytic efficiency, safe, easily recyclable and contribute towards the production of high yields of products in shorter duration of reaction time. Therefore, in our work, zinc ferrite nanoparticles have been chosen as the catalyst for the one pot synthesis of propargyl amine derivatives via A³-coupling reaction. Further, the same catalyst is successfully employed for synthesis of NH-1,2,3-triazoles.

2. Preparation of the catalyst and characterization

ZnFe₂O₄ nanoparticles were prepared by following a literature report [16]. Initially, the precursors zinc oxalate and ferrous oxalate were synthesized. For the synthesis of zinc oxalate, equimolar amount of ZnSO₄·7 H₂O (2.87 g, 10 mmol) and oxalic acid (1.26 g, 10 mmol) were separately dissolved in distilled water and the homogeneous solutions of these two were mixed through vigorous stirring to form white precipitate of zinc oxalate dihydrate. The mixture was filtered to separate the mother liquor and the precipitate was dried in an oven. On the other hand, ferrous oxalate was prepared by initially mixing equimolar aqueous solution of ferrous ammonium sulphate hexahydrate (3.77 g in 12.5 ml) with aqueous solution of oxalic acid (1.67 g in 16.75 ml). The

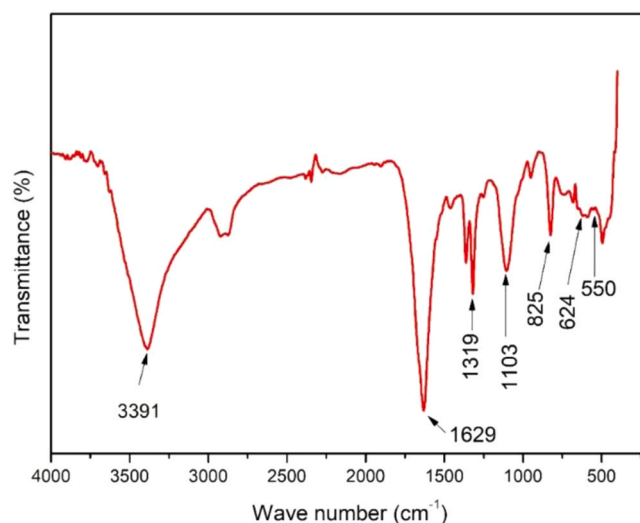


Fig. 4. FTIR spectrum of ZnFe₂O₄.

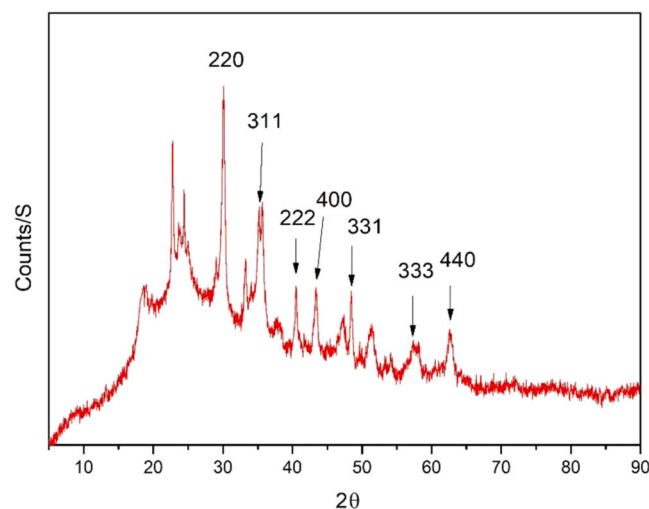


Fig. 5. XRD pattern of ZnFe₂O₄.

mixture was carefully heated to boiling and the yellow granular precipitate formed was allowed to settle. The supernatant liquid was decanted and the precipitate was washed with hot water for several times and oven dried overnight.

The zinc ferrite nanoparticles were then prepared by heating zinc oxalate, ferrous oxalate and PEG600 in weight ratio 1:1:5 under Bunsen burner in open air. After complete burning, the carbon residue from PEG got removed from the mixture as carbon dioxide and the residue left was obtained as zinc ferrite nanoparticles. The final product was then characterized by Scanning Electron Microscopy (SEM), Transmission Electron Microscopy (TEM) and X-Ray Diffraction (XRD) analyses and for the magnetic hysteresis, Vibrating Sample Magnetometer (VSM) was performed.

3. Results and discussion

The surface morphology of the catalyst was studied by SEM analysis and some flake like structures of the particles were obtained as shown in Fig. 1(A) and (B).

TEM analysis confirmed the formation of zinc ferrite nanoparticles (Fig. 2(a) and (b)). The sizes of the nanocrystals were obtained by size counting from the relevant TEM images and it was found that the size of

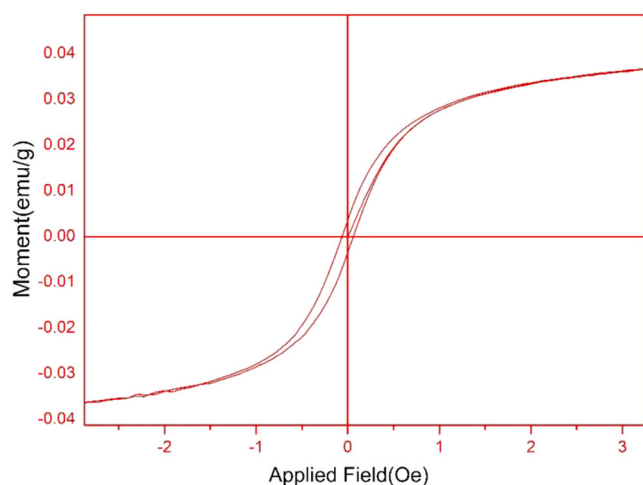


Fig. 6. MH spectrum of fresh catalyst.

the nanoparticles falls in the range of 10–20 nm. HRTEM images (Fig. 2c and d) and SAED pattern (Fig. 3) for the corresponding ferrite nanocrystals portrayed highly crystalline characteristics. The lattice in the image is indexed to the projected (220) plane of the cubic spinel structure of zinc ferrite [17].

Fourier transform infrared (FTIR) analysis of the catalyst was also performed for the prepared catalyst (Fig. 4). The peaks at 624 and 550 cm^{-1} correspond to the vibrational modes of Fe–O stretching and corroborate the spinel structure characteristics of zinc ferrite [16,18]. The peaks at 3391 and 1629 cm^{-1} correspond to water of hydration. The peaks at 1319 and 825 are due to Zn–O–Fe stretching vibrations [19]. The absorption band at 1103 cm^{-1} is due to overtone.

The powder XRD analysis of the synthesized catalyst was also performed (Fig. 5). The reflection at 2θ values 30.1°, 35.1°, 43.4°, 57.3°, 62.5° correspond to the Bragg's planes (220), (311), (400), (333) and (440) which established the formation of FCC cubic spinel structure with the space group of Fd3m (227) of zinc ferrite nanoparticles.

As our concern was to prepare magnetic nanoparticles, the vibrating

sample magnetometer (VSM) analysis was performed for preliminary magnetic measurements. The nature of the magnetic hysteresis (MH) graph confirmed the formation of the ferrite particles with ferromagnetic properties (Fig. 6). The MH graph was measured at 25 °C in the range of $H = \pm 10$ kOe for the fresh catalyst. The saturation magnetization (Ms) at room temperature was found to be 4.5295 emu/g, retentivity (Mr) was equal to 0.35136 emu/g and coercivity (Hci) was 61.175 Oe.

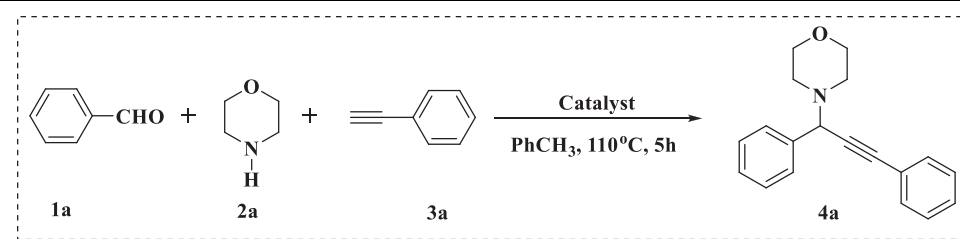
ICP-MS analysis of the catalyst revealed that 7 mg of the fresh catalyst contains 2.78 mol% of Zn which was quite comparable with the theoretical results (2.89 mol% in 7 mg fresh catalyst). Herein, 5 mol% of zinc ferrite (12 mg of the catalyst) was used which contains 4.77 mol% of elemental Zn.

After characterization of the catalyst, it was applied in A^3 -coupling reaction as well as NH-triazole synthesis. The study was initiated by following the multicomponent synthetic procedure with benzaldehyde (1 mmol), morpholine (1.2 mmol) and phenyl acetylene (1.5 mmol) as the model substrates for A^3 coupling. The reaction was set up in a reflux condenser at 110 °C using toluene as the reaction medium and different zinc catalysts along with the precursors of the zinc ferrite were investigated as the catalytic system. With 10 mol% of catalyst loading, it was found that best result was obtained in case of ZnFe_2O_4 compared to other examined catalysts. The precursors of zinc ferrite namely zinc oxalate and iron oxalate gave 77% and 27% of product yields respectively (Table 1, entries 5–6). ZnFe_2O_4 was chosen over them owing to the possession of magnetic properties, better reusability and better productivity.

The amount of the catalyst was optimized (Table 1, entries 7–8, 10–12) and found that 5 mol% of the catalyst loading was enough to carry out the reaction very smoothly.

To find out the best solvent, different types of solvents such as polar, non-polar and green solvents were employed but promising results were obtained only in non-polar solvents especially in toluene which is indeed considered as an excellent organic solvent [20]. Toluene is less toxic than benzene and xylene and only a long time exposure can lead to unhealthy situation. Under reflux condition, in toluene; the model reaction afforded up to 95% product yield in a time duration of 5 h. (Table 2).

Table 1
Optimization of catalyst^a.



Sl. No.	Catalyst	Amount (mol%)	(%)Yield ^b
1	Zn dust	10	64
2	Fe powder	10	58
3	$\text{SiO}_2\text{-Fe(ac)}$	10	30
4	Clay zinc	10	65
5	Zinc oxalate	10	77
6	Fe oxalate	10	27
7	Zinc ferrite	10	96
8	Zinc ferrite	5	95
9 ^c	Zinc ferrite	5	66
10	Zinc ferrite	2	70
11	Zinc ferrite	3	79
12	Zinc ferrite	7	95

^a Reaction conditions: Benzaldehyde (0.106 g, 1 mmol), morpholine (0.104 g, 1.2 mmol) and phenyl acetylene (0.159 g, 1.5 mmol) were refluxed in toluene (2 ml) for 5 h with different catalysts.

^b Isolated yield.

^c Neat condition. (10 mol% = 0.024 g, 7 mol% = 0.016 g, 5 mol% = 0.012 g, 3 mol% = 0.0072 g, 2 mol% = 0.0048 g).

Table 2
Solvent optimization^a.

Sl. No.	Solvent	Temperature (° C)	Yield ^b (%)
1	PEG400	100	–
2	Water	100	–
3	Ethyl acetate	70	–
4	Ethanol	70	–
5	Acetonitrile	80	–
6	THF	65	–
7	DMSO	100	–
8	Hexane	68	42
9	1,4-Dioxane	100	38
10	DMF	100	–
11	Toluene	110	95
12	Chloroform	60	78

^a Reaction conditions: Benzaldehyde (0.106 g, 1 mmol), morpholine (0.104 g, 1.2 mmol) and phenyl acetylene (0.159 g, 1.5 mmol) were refluxed in the respective boiling temperature (except DMF, DMSO, PEG) of the solvents (2 ml) for 5 h.

^b Isolated yield.

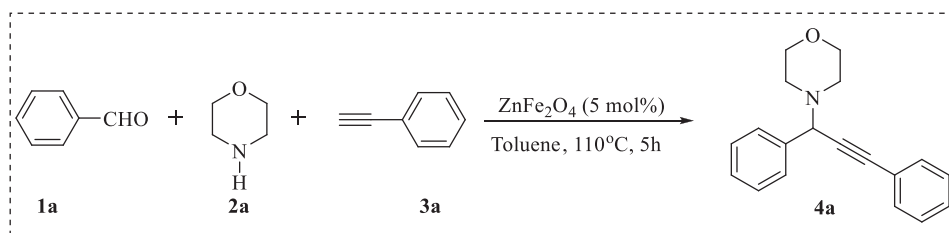
Table 3
Temperature optimization^a.

Sl. No.	Temperature	Yield ^b (%)
1	110	95
2	100	90
3	90	85
4	85	78
5 ^c	90	87

^a Reaction conditions: Benzaldehyde (0.106 g, 1 mmol), morpholine (0.104 g, 1.2 mmol) and phenyl acetylene (0.159 g, 1.5 mmol) were refluxed in toluene (2 ml) for 5 h.

^b Isolated yield.

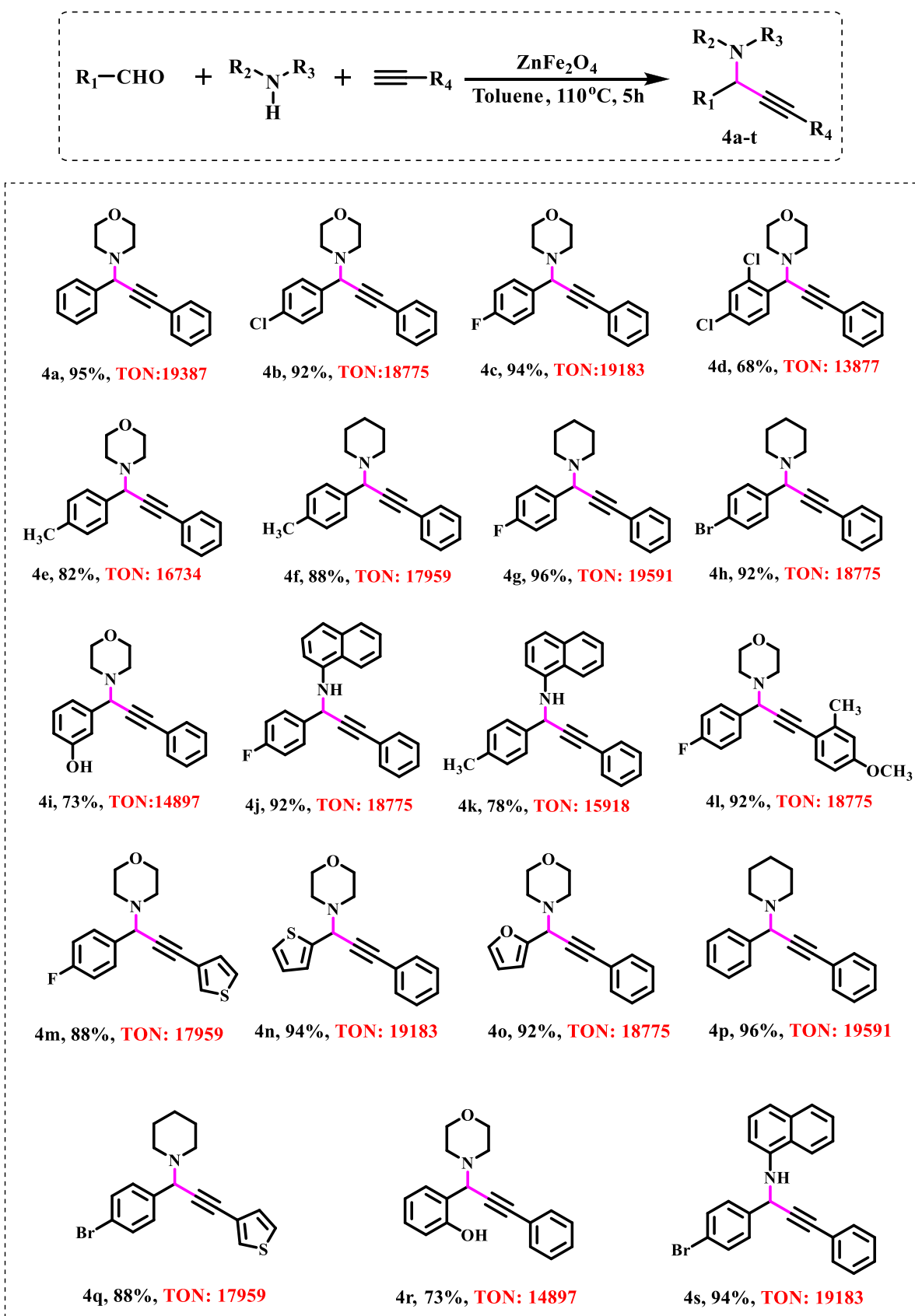
^c Catalyst loading is 5 mol%.

**Scheme 1.** Optimized reaction condition for propargyl amine synthesis.

With the optimized catalyst and solvent, we tried to improve the reaction condition by optimizing the reaction temperature. Variation of the temperature indicated that decrease in the reaction temperature declined the product yield. While employing higher temperature more

than 110 °C did not add any further improvement in product yields. Therefore, 110 °C was set as the ideal temperature to carry out A³-coupling reaction. (Table 3).

Finally we got the best reaction condition as depicted in Scheme 1.

Fig. 7. Substrate scope for propargyl amine derivatives^a.

^aReaction conditions: Aldehyde (1 mmol), amine (1.2 mmol) and alkyne (1.5 mmol) were refluxed in toluene for 5 h. All yields are reported as isolated yields. TON: mmol of product per mmol of catalyst.

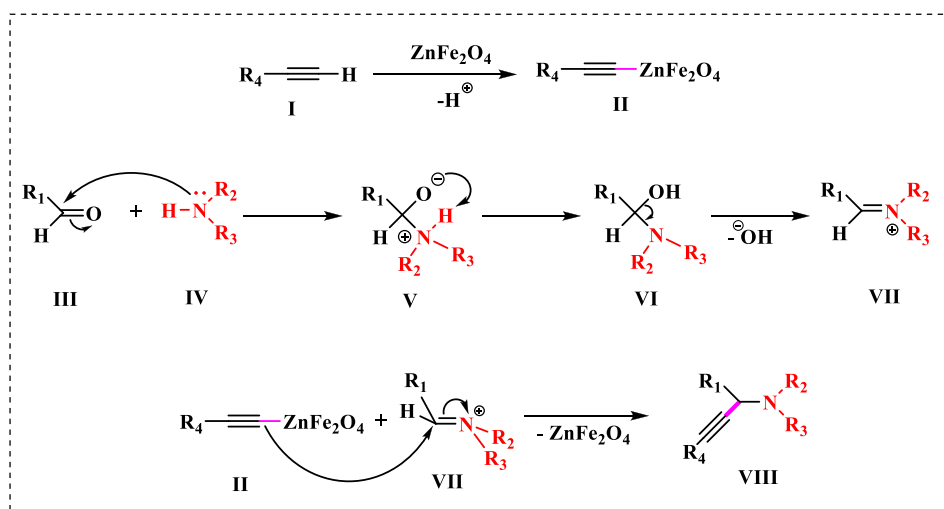
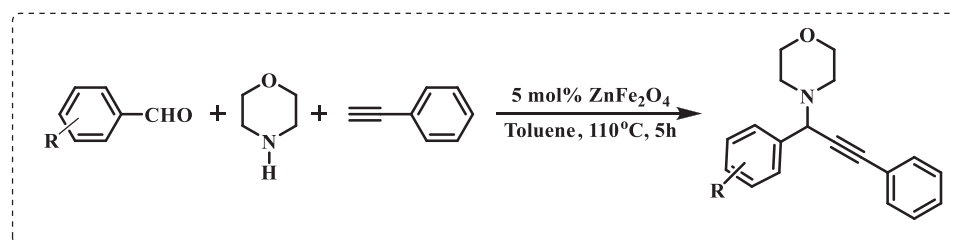


Fig. 8. Plausible mechanistic pathway of the reaction.

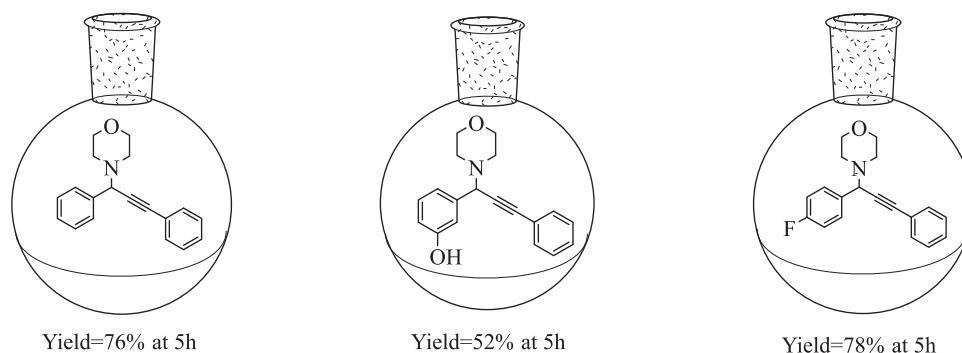
Table 4
Gram scale synthesis^a.

Sl. No.:	Aldehyde	Amine	Alkyne	%Yield ^b
1	Benzaldehyde (1 g, 9.42 mmol)	Morpholine (0.984 g, 11.30 mmol)	Phenyl acetylene (1.499 g, 14.13 mmol)	76
2	3-Hydroxybenzaldehyde (1 g, 8.18 mmol)	Morpholine (0.854 g, 9.81 mmol)	Phenyl acetylene (1.254 g, 12.27 mmol)	52
3	4-Fluorobenzaldehyde (1 g, 8.05 mmol)	Morpholine (0.841 g, 9.66 mmol)	Phenyl acetylene (1.232 g, 12.07 mmol)	78

^a Reaction conditions: Aldehyde (1 equiv), morpholine (1.2 equiv) and phenyl acetylene (1.5 equiv) were refluxed in toluene at 110 °C for 5 h with 5 mol% ZnFe₂O₄.
^b Isolated yields.

To justify the optimized reaction protocol, we extended our study by the variation of different starting materials and results are summarized in Fig. 7. From the results, it is quite noticeable that the presence of halogen in the aldehyde counterpart facilitates the reaction very smoothly (Fig. 7, entries 4b-4-c, 4 h-4-i, 4 l-4-m, 4o-4-p), whereas the aldehydes with electron donating group slow down the kinetics of the reaction (Fig. 7, entries 4e, 4 f, 4 g, 4 n, 4q). Unlike previous literatures, we observed quite a decent yield of 82% with 4--methyl benzaldehyde (Fig. 7, entry 4e). The yield of the product is low in case of disubstituted

aldehyde (Fig. 7, entry 4d) which may be due to the steric crowding in the desired product. The reaction condition also showed excellent tolerance towards heterocyclic aldehydes. To extend the applicability of the protocol, variation in amine as well as alkyne components was also performed. Morpholine, piperidine and naphthyl amine were employed in this regard and quantitative yields were obtained. The feasibility of the reaction is found to be low only in case of aliphatic alkynes, aliphatic aldehydes and simple amines like diethyl amine and ethyl amine.



Scheme 2. Schematic representation of the gram scale synthesis of propargyl amine.

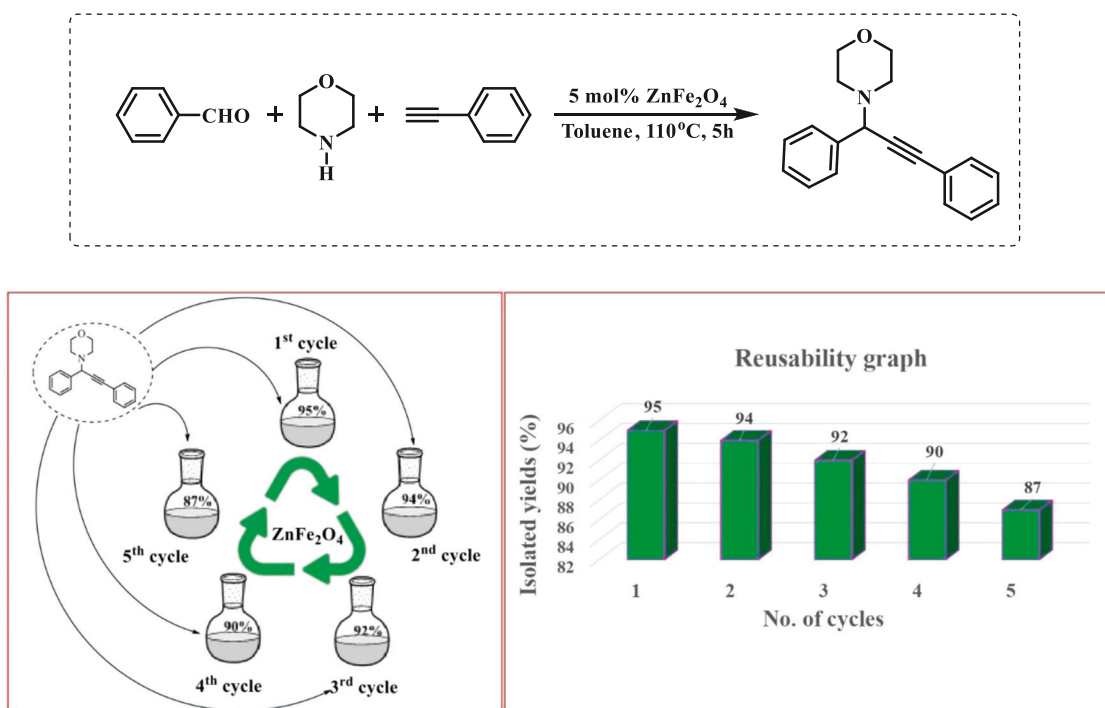


Fig. 9. Reusability of the catalyst: schematic as well as graphical representations^a.

^aReaction conditions: Benzaldehyde (1 equiv), morpholine (1.2 equiv) and phenyl acetylene (1.5 equiv) were refluxed in toluene at 110 °C for 5 h with 5 mol% ZnFe₂O₄. Isolated yields are reported.

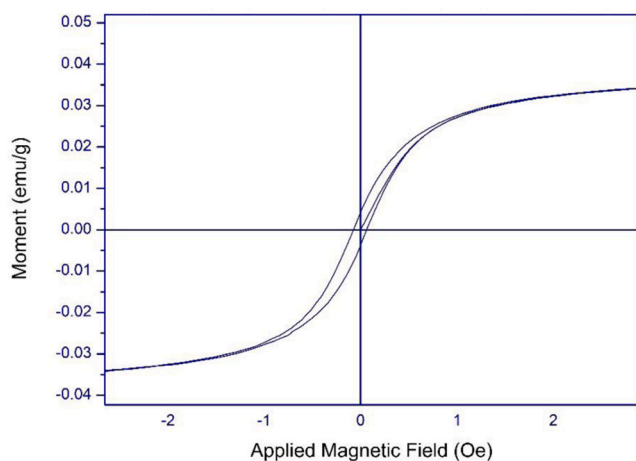


Fig. 10. MH spectra of the reused catalyst.

3.1. Reaction pathway

In this protocol, initially discrete formation of acetylide (II) and imine (VII) takes place from their respective starting materials (Fig. 8). The lone pair on nitrogen attacks the electrophilic carbon atom of the aldehyde to get the intermediate V followed by intramolecular proton transfer to obtain intermediate VI. This intermediate loses a hydroxyl group to form the imine intermediate VII. The acetylide then attacks the electrophilic carbon atom of the imine intermediate VII to give the desired product VIII. The catalyst is regenerated in the final step and is ready for the next cycle [9(b),21].

Further, to demonstrate the synthetic utility of this protocol, three gram-scale reactions were carried out by using three different combinations as shown in Table 4.

The schematic representations of the results are shown in Scheme 2.

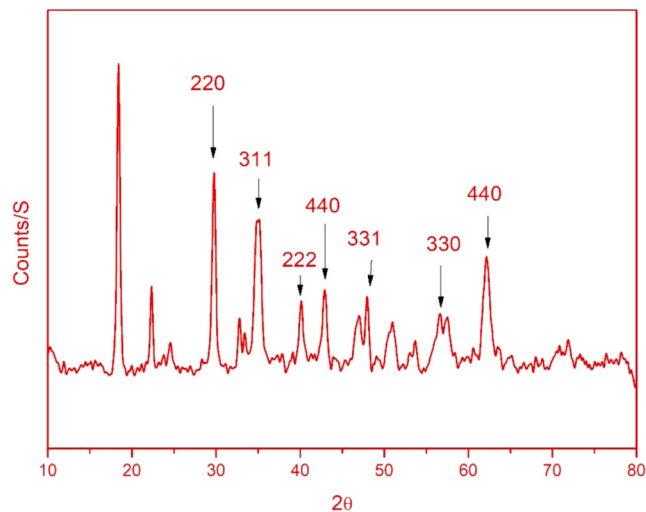


Fig. 11. X-ray diffraction pattern of the reused catalyst.

3.2. Reusability

For further determination of the catalytic efficiency, we thought of reusing the catalyst by recovering it from the reaction mixture and it was observed that the catalyst can successfully be applied up to 5th catalytic cycle with negligible loss in the product yield. In doing so, we have chosen benzaldehyde, morpholine and phenyl acetylene as the model substrates. After the fresh batch of reaction, the catalyst was separated by means of magnetic separation followed by centrifugation to ensure maximum possible recovery of the catalyst. The catalyst was dried and again applied to another cycle by maintaining the same stoichiometry of the reaction. This process was repeated for five consecutive cycles. Both schematic and graphical representations of this process are presented in

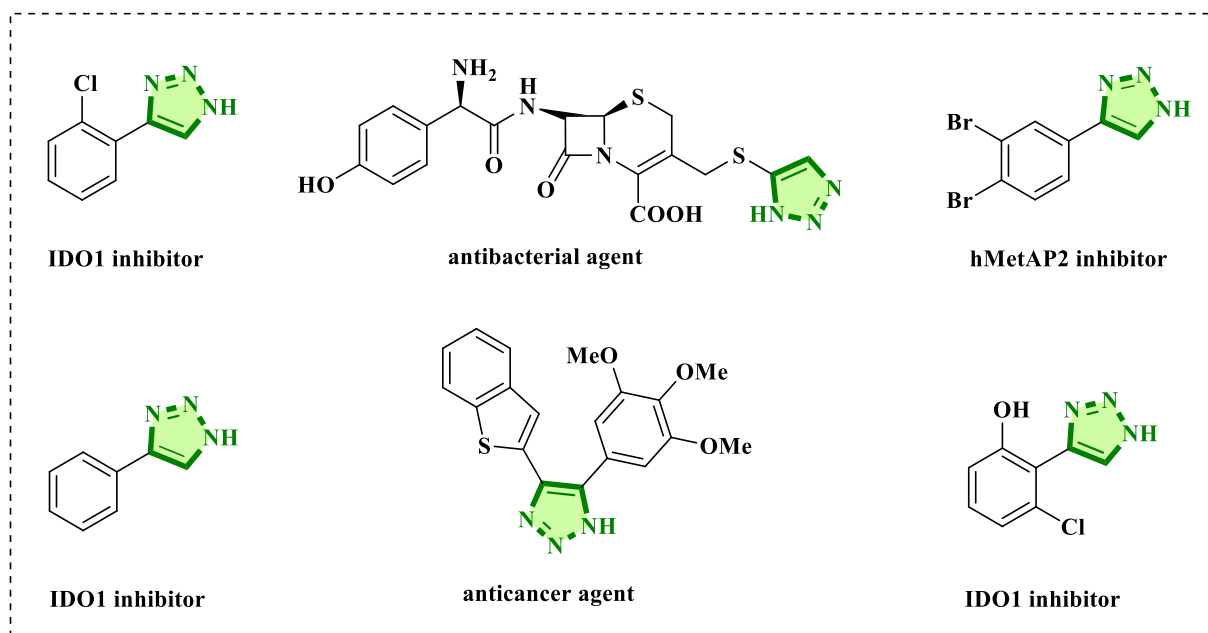


Fig. 12. NH-triazole containing biologically active molecules.

Table 5
Optimization of reaction parameters^a.

Sl. NO.:	Temperature (°C)	Solvent	% Yield ^b
1	70	H ₂ O	trace
2	70	Ethyl acetate	trace
3	70	Ethanol	trace
4	70	Toluene	–
5	70	THF	–
6	70	Ethyl-L-Lactate	34
7	70	PEG	50
8	100	PEG	93
9	110	PEG	93
10	100	Neat	–
11	70	H ₂ O + PEG (1:1)	40
12	90	H ₂ O + PEG (1:1)	76
13	100	H ₂ O + PEG (1:1)	79
14	110	H ₂ O + PEG (1:1)	81
15	100	H ₂ O + PEG (50 μL)	68
16	100	H ₂ O + PEG (100 μL)	71
17	100	H ₂ O + PEG (200 μL)	73
18 ^c	100	PEG	78
19 ^d	100	PEG	94
20 ^e	100	PEG	33
21 ^f	100	PEG	86
22 ^g	100	PEG	93

^a Reaction conditions: Benzaldehyde(1 mmol), nitromethane (1.5 mmol) and NaN₃ (2 mmol) were heated in PEG400 for 4 h with zinc ferrite (5 mol%), Solvent (2 ml).

^b Isolated yield.

^c 2 mol% of the catalyst was used.

^d 10 mol% of the catalyst was used.

^e Reaction was performed in absence of the catalyst.

^f 3 mol% of the catalyst was used.

^g 7 mol% of the catalyst was used.

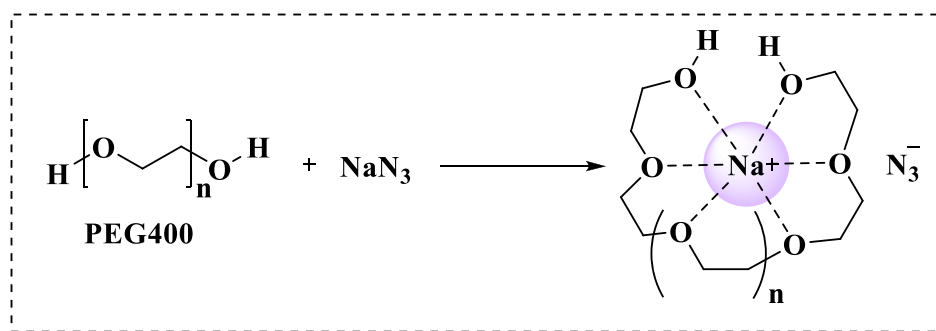


Fig. 13. Schematic representation of PEG400 acting as crown ether.

Fig. 9.

After reusing up to 5th times, VSM analysis was again performed for the reused catalyst (Fig. 10) and almost similar values were obtained which is an indication that the prepared catalyst retained its magnetism after reuse. The values found for the reused catalyst were 68.148 Oe, 4.0036 emu/g, 0.39648 emu/g as coercivity (H_{ci}), magnetization (M_s) and retentivity (M_r) respectively.

XRD analysis was also performed to the reused catalyst and almost identical pattern was observed which suggests that the catalyst remained unaltered during the reaction (Fig. 11).

3.3. Application of zinc ferrite in NH-1,2,3-triazole synthesis

4-Aryl-NH-1,2,3-triazoles are recognized as important class of 1,2,3-triazoles and receive tremendous attention for years due to their numerous biological properties [22]. The bio-isosteric nature of the triazole molecules with the amide bond makes them privileged molecular entity for successful exploitation in medicinal chemistry such as anticancer drugs [23], antibacterial and antibiotic agents along with as a suitable probe for the biosynthesis of endocannabinoid [24] (Fig. 12).

Compared to the N-substituted triazoles, the synthesis of N-unsubstituted triazoles is fairly challenging, with few methods available which are based on metal catalysis [25], 1,3-dipolar cycloaddition [26], multicomponent reaction [27], organocascade process [28] and heterogeneous catalyst. Despite of having prevailing importance, these methods own several demerits like limited substrate scope, inaccessible starting materials and harsh reaction conditions. Therefore, there is scope for development of improved method for NH-triazole synthesis and hence in this work, along with the A^3 coupling reaction; we have tried to synthesize the NH-triazoles by applying zinc ferrite as the catalytic system. With this catalyst NH-triazole synthesis proceeded smoothly from the starting materials aldehyde, nitroalkane and NaN_3 again via one pot strategy.

4. Results and discussion

For the optimization of NH-triazole synthesis, different solvent systems were examined with 5 mol% of zinc ferrite as the catalyst at different temperatures. Water being an inexpensive, cheap and non-toxic medium [29], was screened as the first choice for the reaction but no positive outcome was observed (Table 5, entry 1). Some polar (Table 5, entries 2–3) and non-polar (Table 5, entries 4–5) solvents were also part of this investigation but neither of them stood high in this context. After obtaining disappointing results with these solvent systems, green solvent ethyl-L-lactate was used which also showed ineffectiveness towards triazoles synthesis (Table 5, entry 6). Further, we opted for PEG 400 and surprisingly 93% of product yield was obtained in PEG 400 within 4 h at 100 °C (Table 5, entry 8). After getting optimistic results in PEG400, the study was extended by using various solvent mixtures comprising of PEG 400 and water in different proportion

(Table 5, entries 11–17) at different temperatures but these combinations also failed to display superior reactivity to PEG400 alone. It may be due to the polymeric nature of PEG400, it can enhance the solubility of the organic compounds. Moreover, PEG400 can act as a crown ether [30] as well as a phase transfer agent [31] which in turn enhances the solubility of metal-based salts such as sodium azide (Fig. 13). Due to all these factors, the reaction might occur in the same phase which in turn facilitated the reaction. Thereafter the catalyst loading was changed to 2 mol% (Table 5, entry 18) and 10 mol% (Table 5, entry 19) respectively but none of them exhibited superior activity to the results obtained when 5 mol% of the catalyst was used. Further, we have also performed two more reactions with 3 mol% (Table 5, entry 21) and 7 mol% (Table 5, entry 22) catalyst loading. No further improvement in yield was observed with 7 mol% catalyst and a decrease in yield was observed with 3 mol% catalyst. Another reaction without catalyst was also performed. The uncatalyzed reaction afforded 33% product yield which is believed to be due to the presence of thermal energy. Hence 5 mol% of the catalyst was considered optimum for catalytic action. After obtaining best condition, different aryl aldehydes were tested with nitromethane/nitroethane and NaN_3 to generate NH-1,2,3-triazoles in good to excellent yields. The results are summarized in Table 6.

4.1. Synthesis of biologically active NH-triazole molecule in large scale

As our method was able to tolerate a wide range of substrate scope, we thought of applying our method for the synthesis of medically established NH-triazole molecules in larger scale and fruitful results were obtained thereby making our method as an efficient one. The observation are incorporated in Table 7.

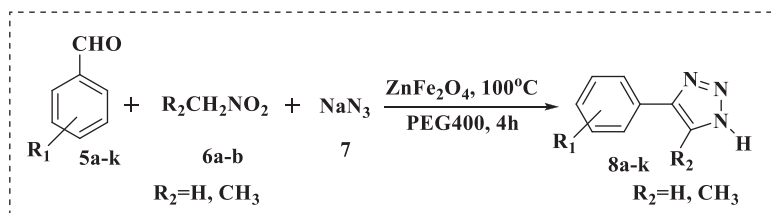
4.2. Mechanism of action

The reaction proceeds with the formation of nitroalkene (III) from aldehyde and nitroalkane (Fig. 14). Due to the Lewis acidic nature of Zn (II), zinc ferrite attacks the nucleophilic oxygen atom of the nitro group (IV). Then NaN_3 attacks the electrophilic double bond of the intermediate V followed by subsequent cyclization. Zinc ferrite is then detached followed by expulsion of nitro group providing aromaticity to the compound which may act as the driving force for the forward reaction to obtain intermediate VIII. Protonation to this intermediate finally gives the desired molecule IX [33].

Further, to validate the plausible mechanism, we have performed computational study. To the best of our knowledge, it is the first report on the theoretical study on the mechanism of NH-1,2,3-Triazole. The details of the study are stated below:

All the structures were fully optimized without any symmetry constraints in the gas phase and at 298 K using M06–2X/Def2-TZVP level of theory [34]. Harmonic frequency calculations were also performed at the same level of theory to understand the nature of the stationary states. All intermediates and products were found to be at their local minima

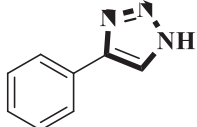
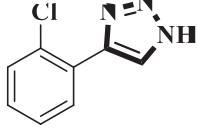
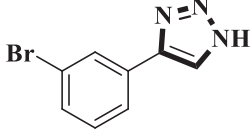
Table 6
Substrate scope^a.



Entry	Aldehyde	Nitroalkane	Product	Yield	TON
1		CH ₃ NO ₂		93%	18979
2		CH ₃ NO ₂		88%	17959
3		CH ₃ NO ₂		68%	13877
4		CH ₃ NO ₂		87%	17755
5		CH ₃ NO ₂		92%	18775
6		CH ₃ NO ₂		90%	18367
7		CH ₃ NO ₂		89%	18163
8		CH ₃ NO ₂		79%	16122
9		CH ₃ NO ₂		78%	15918
10		CH ₃ CH ₂ NO ₂		88%	17959
11		CH ₃ CH ₂ NO ₂		88%	17959

^a Reaction conditions: Aldehyde (1 mmol), nitroalkane (1.5 mmol) and NaN₃ (2 mmol) were heated in 2 ml PEG400 for 4 h with Zinc ferrite (5 mol%). All the yields reported here are isolated yields.

Table 7
Synthesis of previously existing biological molecule.

Sl. No.:	Aldehyde	Product	%Yield ^b	Activity
1	Benzaldehyde (1 g, 9.42 mmol)		82	IDO1 inhibitor[32(a)]
2	2-Chlorobenzaldehyde 1 g, 8.18 mmol		78	IDO1 inhibitor[32(a)]
3	3-Bromobenzaldehyde (1 g, 8.05 mmol)		79	hMETAP2 inhibitor[32(b)]

^aReaction conditions: Aldehyde (1 equiv), nitromethane (1.5 equiv) and NaN_3 (1.5 equiv) were heated in PEG400 at 100 °C for 4 h with 5 mol% ZnFe_2O_4 .

^b Isolated yields.

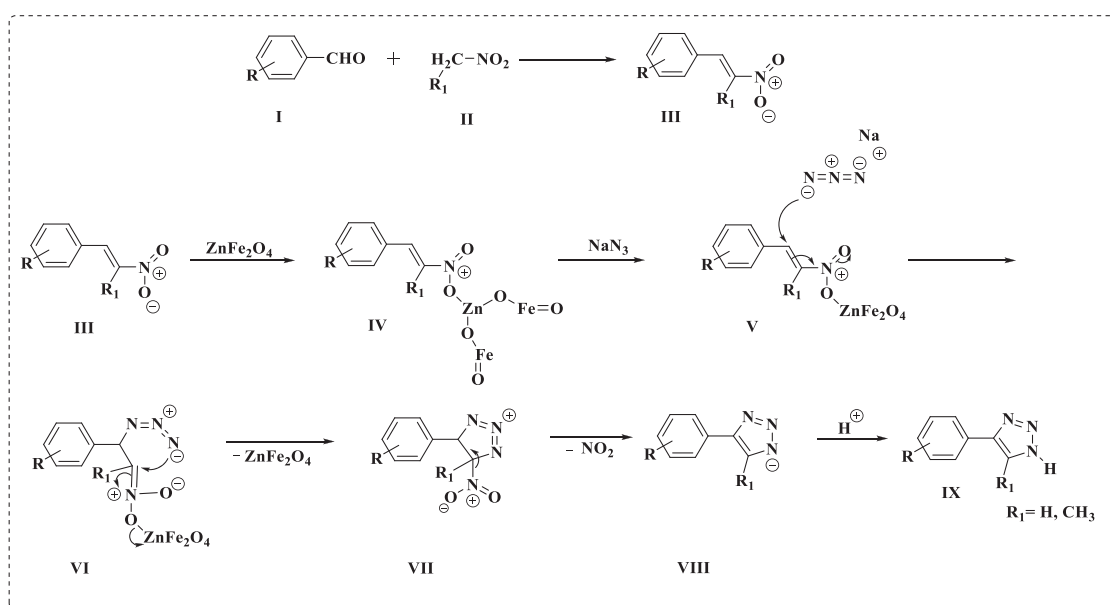


Fig. 14. Plausible mechanistic steps of formation of NH-1,2,3-Triazole.

with all real frequencies while the transition state was found to have one imaginary value of the frequency corresponding to the movement of the terminal N-atom of the N_3^- group to the terminal acyclic carbon atom. Further, the transition state was verified with intrinsic reaction coordinate analysis. All energies are zero point and thermally corrected. All calculations were performed using GAUSSIAN16 suite of program [35].

In the first step of the mechanism (Fig. 15), ZnFe_2O_4 attaches to the $-\text{NO}_2$ group of A through one of the O-atoms to generate B. This step is calculated to be exergonic by 3.2 kcal/mol. In the next step, azide ion,

N_3^- attacks the olefinic carbon atom which bears a positive natural charge of 0.45 |e|. The formation of C through this step is also found to be exergonic by 1.3 kcal/mol. C then loses ZnFe_2O_4 to generate the final N-heterocyclic product D through the transition state TS_{CD} . The activation barrier involved in this process is moderate, only 8.7 kcal/mol at this level of theory. The $\text{C}\cdots\text{N}$ distance in TS_{CD} is 1.913 Å. The loss of NO_2 and a proton yields the final product D. This process is again exergonic by 4.5 kcal/mol. The overall exergonic nature of the process with a moderate activation barrier is expected to help the formation of the N-

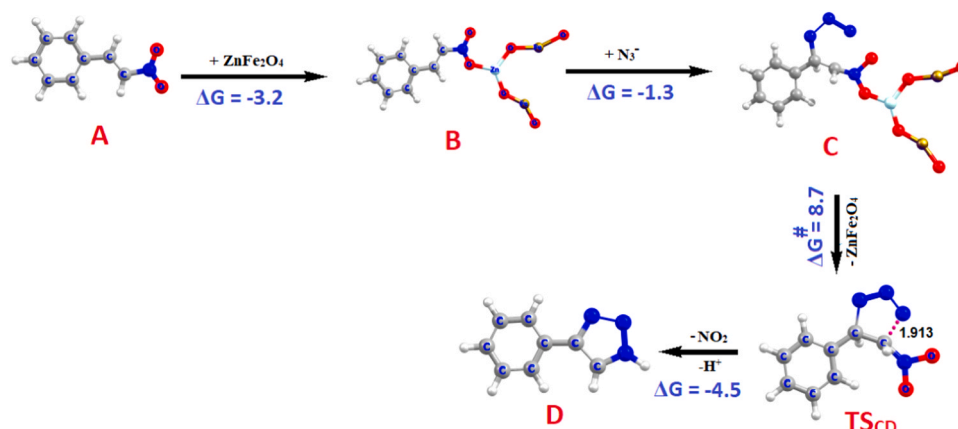


Fig. 15. Energetic of the reaction profile. All relative energies are in kcal/mol and are zero point and thermally corrected. Bond length is in Å.

Table 8

Comparison of the present protocol of A³ coupling with some literature reports.

Entry	Conditions	Yield (%)	References
1	CuFe ₂ O ₄ (6.5 mol%), toluene, 80 °C, N ₂ , 4–15 h	65–91%	[36(a)]
2	Fe ₃ O ₄ MNPs (20 mol%), toluene, 80–110 °C, 16 h	40–92%	[36(b)]
3	Fe ₃ O ₄ @SBA-15 (5 mol%), toluene, 110 °C, 6–8 h	45–93%	[36(c)]
4	MNP@PILAu (5 mg), 10–20 h	86–98%	[36(d)]
5	Fe ₃ O ₄ @Au NPs (10 mol%), toluene, 100 °C, 48 h	7–95%	[36(e)]
6	ZnFe ₂ O ₄ , toluene, 100 °C, 5 h	68–96%	This work

heterocyclic product both thermodynamically and kinetically.

4.3. Brief comparison

Herein, we have reported two separate synthetic procedures to access propargyl amine as well as NH-triazole catalysed by the same catalyst zinc ferrite. Both these class of compounds possess their own importance regarding chemical, medicinal and industrial fields. Propargyl amines can be exceptionally useful as intermediates to the synthesis of various heterocyclic compounds. Moreover, some of their derivatives can be used as effective remedies for Parkinson's as well as Alzheimer diseases. On the other hand, NH-triazoles offer a variety of important compounds having various pharmacophoric attributes e.g. anti-inflammatory, antiviral, antibacterial etc. Here, in our approach, both the reactions provided exciting results in their respective developed methodologies. In case of propargyl amine synthesis, toluene provided the suitable medium whereas in case of NH-triazoles, this job was done by PEG400. As discussed earlier, along with the organic compounds metal based salts are easily soluble in PEG due to its ability to act as crown ether. The presence of NaN₃ as one of the starting materials has better solubility in PEG400 by the formation of crown ether. However, we believe that lack of similar salt like starting material for the synthesis of propargyl amine restricts the aforementioned reaction in PEG400. Moreover, In order to highlight the efficiency of the present protocol of A³ coupling, our results are compared with some literature reports in Table 8.

5. Conclusions

In this work, we have demonstrated an efficient methodology for both A³-coupling as well as NH-1,2,3-triazole synthesis. The affordability of the starting materials as well as precursors of the catalyst, the inertness of the catalyst to the environment, magnetic separation and chemical reactivity are the positive outcomes of the described

methodology. To the best of our knowledge, only a few reports are available citing use of zinc catalyst in A³-coupling as well as NH-triazole synthesis and none describes use of zinc ferrite. We therefore, hope our catalytic system can be used as an effective alternative for propargyl amine as well as NH-triazole synthesis.

Supporting Information

General Information, Experimental and Analytical data, ¹H and ¹³C NMR spectra and characterization data all are found in the "Supplementary Content" section of this article's webpage.

CRediT authorship contribution statement

Roktopol Hazarika: Conceptualization, Visualization, Formal analysis, Data curation, Writing – original draft. **Anirban Garg:** Data curation, Visualization. **Swadhin Chetia:** Formal analysis. **Parmita Phukan:** Formal analysis. **Akshay Kulshrestha:** Formal analysis, Data curation. **Arvind Kumar:** Formal analysis. **Ankur Bordoloi:** Formal analysis, Data curation. **Amlan Jyoti Kalita:** Formal analysis, Data curation. **Ankur Kanti Guha:** Formal analysis, Data curation. **Diganta Sarma:** Conceptualization, Supervision, Writing – review & editing, Visualization.

Declaration of Competing Interest

The authors declare that they have no known competing financial interests or personal relationships that could have appeared to influence the work reported in this paper.

Acknowledgements

D.S. is thankful to DST, New Delhi, India for a research grant [No. EMR/2016/002345]. Authors thank the Department of Science and Technology for financial assistance under DST-FIST programme and UGC, New Delhi for Special Assistance Programme (UGC-SAP) to the Department of Chemistry, Dibrugarh University.

Appendix A. Supporting information

Supplementary data associated with this article can be found in the online version at doi:10.1016/j.apcata.2021.118338.

References

- (a) A. Domling, I. Ugi, *Angew. Chem. Int.* 112 (2000) 3300–3344;
(b) I. Ugi, A. Domling, B. Werner, *J. Heterocycl. Chem.* 37 (2000) 647–658;

- (c) R.W. Armstrong, A.P. Combs, P.A. Tempst, S.D. Brown, T.A. Keating, *Acc. Chem. Res.* 29 (1996) 123–131.
- [2] T. Harada, T. Fujiwara, K. Iwazaki, A. Oku, *Org. Lett.* 2 (2000) 1855.
- [3] (a) C. Wei, C.J. Li, *J. Am. Chem. Soc.* 125 (2003) 9584;
(b) L. Shi, Y.Q. Tu, M. Wang, F.M. Zhang, C.A. Fan, *Org. Lett.* 6 (2004) 1001;
(c) N. Gommermann, C. Koradin, K. Polborn, P. Knochel, *Angew. Chem. Int. Ed.* 42 (2003) 5763;
(d) F. Colombo, M. Benaglia, S. Orlandi, F. Uselli, *J. Mol. Catal. A: Chem.* 260 (2006) 128;
(e) A. Bisai, V.K. Singh, *Org. Lett.* 8 (2006) 2405;
(f) K.Y. Lee, C.G. Lee, J.E. Na, J.N. Kim, *Tetrahedron Lett.* 46 (2005) 69;
(g) L. Zani, S. Alesi, P.G. Cozzi, C. Bolm, *J. Org. Chem.* 71 (2006) 1558;
(h) T. Murai, Y. Mutoh, *Chem. Lett.* 41 (2012) 2–8.
- [4] (a) M. Gholinejad, M. Afrasi, C. Najera, *Appl. Organomet. Chem.* 33 (2019), e4760;
(b) M. Gholinejad, F. Zareh, C. Najera, *Appl. Organomet. Chem.* 32 (2018), e4454;
(c) M. Gholinejad, R. Bonyasi, C. Najera, F. Saadati, M. Bahrami, N. Dasvarz, *ChemPlusChem* 83 (2018) 431–438;
(d) M. Gholinejad, F. Hamed, C. Najera, *Synlett* 27 (2016) 1193–1201;
(e) M. Gholinejad, F. Saadati, S. Shaybanizadeh, B. Pullithadathil, *RSC Adv.* 6 (2016) 4983–4991;
(f) M. Gholinejad, B. Karimi, A. Aminianfar, M. Khorasani, *ChemPlusChem* 80 (2015) 1573–1579.
- [5] (a) B. Ringdahl, in: J.H. Brown (Ed.), *The Muscarinic Receptors*, Humana Press, Clifton NJ, 1989;
(b) M. Miura, M. Enna, K. Okuro, M. Nomura, *J. Org. Chem.* 60 (1995) 4999–5004;
(c) A. Jenmalm, W. Berts, Y.L. Li, K. Luthman, I. Csoregh, U. Hacksell, *J. Org. Chem.* 59 (1994) 1139–1148;
(d) G. Dyker, *Angew. Chem. Int.*, Ed. 111 (1999) 1808–1822;
(e) J. Ying, Z. Le, Z.P. Bao, X.F. Wu, *Org. Chem. Front.* 7 (2020) 1006–1010.
- [6] J.J. Chen, D.M. Swope, K. Dashtipour, *Clin. Ther.* 29 (2007) 1825–1849.
- [7] M. Naoi, W. Maruyama, M. Shamoto-Nagai, H. Yi, Y. Akao, M. Tanaka, *Mol. Neurobiol.* (2005) 81–93.
- [8] (a) V.A. Peshkov, O.P. Pereshivko, E.V. Van der Eycken, *Chem. Soc. Rev.* 41 (2012) 3790–3807;
(b) S. Srivastava, *New J. Chem.* 43 (2019) 6469–6471.
- [9] (a) Y. Qiu, Y. Qin, Z. Ma, W. Xia, *Chem. Lett.* 43 (2014) 1284–1286;
(b) N.P. Eagalapati, A. Rajack, Y.L.N. Murthy, *J. Mol. Catal. A: Chem.* 381 (2014) 126–131.
- [10] (a) M. Colombo, S. Carregal-Romero, M.F. Casula, L.A.G. Rrez, M.A.P. Morales, D. Proserpi, W.J. Parak, *Chem. Soc. Rev.* 41 (2012) 4306–4334;
(b) Z. Li, J.Y. Zhang, X. Li, H. Guo, Z.Z. Zhang, *J. Pharm. Sci. -Us* 107 (2018) 2694–2701;
(c) S.C. Mohanta, A. Saha, P.S. Devi, *Mater. Today* 5 (2018) 9715–9725;
(d) L. Vekas, M.V. Avdeev, D. Bica, in: D. Shi (Ed.), *Nanoscience Biomedicine*, Springer, Berlin, Germany, 2009, pp. 650–720;
(e) D. Susan-Resiga, V. Socoliuc, T. Boros, T. Borbáth, O. Marinica, A. Han, L. Vékás, *J. Colloid Interface Sci.* 373 (2012) 110–115.
- [11] (a) G. Gao, J.Q. Di, H.Y. Zhang, L.P. Mo, Z.H. Zhang, *J. Catal.* 387 (2020) 39–46;
(b) M.N. Chen, L.P. Mo, Z.S. Cui, Z.H. Zhang, *Curr. Opin. Green. Sustain. Chem.* 15 (2019) 27–37;
(c) M. Zhang, Y.H. Liu, Z.R. Shang, H.C. Hu, Z.H. Zhang, *Catal. Commun.* 88 (2017) 39–44.
- [12] A. Khazaei, A. Ranjbaran, F. Abbasi, M. Khazaeia, A.R. Moosavi, *RSC Adv.* 5 (2015) 13643–13647.
- [13] K. De, C. Mukhopadhyay, *ChemistrySelect* 3 (2018) 6873–6879.
- [14] T.R.R. Naik, S.A. Shivashankar, *Tetrahedron Lett.* 57 (2016) 4046–4049.
- [15] A. Maleki, Z. Varzi, F. Hassanzadeh-Afrouzi, *Polyhedron* 171 (2019) 193–202.
- [16] P.M.P. Swamy, S. Basavaraja, A.K. Lagashetty, N.V.S. Rao, R. Nijagunappa, A. Venkataraman, *Bull. Mater. Sci.* 34 (2011) 1325–1330.
- [17] H. Yoon, J.S. Lee, J.H. Min, J. Wu, Y.K. Kim, *Nanoscale Res. Lett.* 8 (2013) 530.
- [18] R.D. Waldron, *Phys. Rev.* 99 (1955) 1727–1735.
- [19] C.A. Ladole, *Int. J. Chem. Sci.* 10 (2012) 1230–1234.
- [20] (a) S.R. Toluene Clough, *Encycl. Toxicol.* (2005) 202–204;
(b) E.D. Nawawinetu, A.R. Tualeka, *Indian J. Forensic Med. Toxicol.* 13 (2019) 4.
- [21] K.V.V. Satyanarayana, P.A. Ramaiah, Y.L.N. Murty, M.R. Chandra, S.V.N. Pammi, *Catal. Commun.* 25 (2012) 50–53.
- [22] (a) J. Thomas, S. Jana, S. Liekens, W. Dehaen, *Chem. Commun.* 52 (2016) 9236;
(b) L.S. Kallander, Q. Lu, W. Chen, T. Tomaszek, G. Yang, D. Tew, T.D. Meek, G. A. Hofmann, C.K. Schulz-Pritchard, W.W. Smith, C.A. Janson, M.D. Ryan, G. Zhang, K.O. Johanson, R.B. Kirkpatrick, T.H. Ho, P.W. Fisher, M.R. Mattern, R. K. Johnson, M.J. Hansbury, J.D. Winkler, K.W. Ward, D.F. Veber, S.K. Thompson, *J. Med. Chem.* 48 (2005) 5644–5647;
(c) Q. Huang, M. Zheng, S. Yang, C. Kuang, C. Yu, Q. Yang, *Eur. J. Med. Chem.* 46 (2011) 5680–5687;
(d) U.F. Rohrig, S.R. Majjigapu, A. Grosdidier, S. Bron, V. Stroobant, L. Pilotte, D. Colau, P. Vogel, B.J. Van den Eynde, V. Zoete, O. Michielin, *J. Med. Chem.* 55 (2012) 5270–5290.
- [23] (a) L.S. Kallander, Q. Lu, W. Chen, T. Tomaszek, G. Yang, D. Tew, T.D. Meek, G. A. Hofmann, C.K. Schulz-Pritchard, W.W. Smith, C.A. Janson, M.D. Ryan, G. Zhang, K.O. Johanson, R.B. Kirkpatrick, T.F. Ho, P.D. Fisher, M.R. Mattern, R. K. Johnson, M.J. Hansbury, J.D. Winkler, K.W. Ward, D.F. Veber, S.K. Thompson, *J. Med. Chem.* 48 (2005) 5644–5647;
(b) U.F. Rohrig, L. Awad, A. Grosdidier, P. Larrieu, V. Stroobant, D. Colau, V. Cerundolo, A.J.G. Simpson, P. Vogel, B.J. Van den Eynde, V. Zoete, O. Michielin, *J. Med. Chem.* 53 (2010) 1172–1189;
(c) Q. Huang, M. Zheng, S. Yang, C. Kuang, C. Yu, Q. Yang, *Eur. J. Med. Chem.* 46 (2011) 5680–5687;
(d) U. Rohrig, S.R. Majjigapu, A. Grosdidier, S. Bron, V. Stroobant, L. Pilotte, D. Colau, P. Vogel, B.J.V. Eynde, V. Zoete, O. Michielin, *J. Med. Chem.* 55 (2012) 5270–5290.
- [24] (a) L.A. McAllister, J.I. Montgomery, J.A. Abramite, U. Reilly, M.F. Brown, J. M. Chen, R.A. Barham, Y. Che, S.W. Chung, C.A. Menard, M.-F. Mark, L.M. Mullins, M.C. Noe, J.P. Donnell, R.M. Oliver III, J.B. Penzien, M. Plummer, L.M. Price, V. Shanmugasundaram, A.P. Tomaras, D.P. Uccello, *Bioorg. Med. Chem. Lett.* 22 (2012) 6832–6838;
(b) S. Oh, W.-S. Shin, J. Ham, S. Lee, *Bioorg. Med. Chem. Lett.* 20 (2010) 4112–4115;
(c) K.-L. Hsu, K. Tsuboi, L.R. Whitby, A.E. Speers, H. Pugh, J. Inloes, B.F. Cravatt, *J. Med. Chem.* 56 (2013) 8257–8269.
- [25] (a) J. Kalisiak, K.B. Sharpless, V.V. Fokin, *Org. Lett.* 10 (2008) 3171–3174;
(b) A.E. Cohrt, J.F. Jensen, T.E. Nielsen, *Org. Lett.* 12 (2010) 5414–5417;
(c) T. Jin, S. Kamijo, Y. Yamamoto, *Eur. J. Org. Chem.* (2004) 3789;
(d) S. Agarwal, P. Phukan, D. Sarma, K. Deori, *Nanoscale Adv.* 3 (2021) 3954–3966;
(e) P. Phukan, S. Agarwal, K. Deori, D. Sarma, *Catal. Lett.* 150 (2020) 2208–2219;
(f) A. Garg, N. Borah, J. Sultana, A. Kulashetra, A. Kumar, D. Sarma, *Appl. Organomet. Chem.* (2021), e6298.
- [26] (a) J. Barluenga, C. Valdes, G. Beltran, V. Escribano, F. Aznar, *Angew. Chem. Int. Ed.* 45 (2006) 6893–6896;
(b) X. Wang, C. Kuang, Q. Yang, *Eur. J. Org. Chem.* 2 (2012) 424–428;
(c) N.S. Zefirov, N.K. Chapovskaya, V.V. Kolesnikov, *J. Chem. Soc. D* 17 (1971) 1001–1002.
- [27] (a) Q. Hu, Y. Liu, X. Deng, Y. Li, Y. Chen, *Adv. Synth. Catal.* 358 (2016) 1689–1693;
(b) R. Hui, M. Zhao, M. Chen, Z. Ren, Z. Guan, *Chin. J. Chem.* 35 (2017) 1808–1812;
(c) J. Thomas, S. Jana, S. Liekensand, W. Dehaen, *Chem. Commun.* 52 (2016) 9236–9239.
- [28] (a) D.B. Ramachary, K. Ramakumar, V.V. Narayana, *Chem. Eur. J.* 14 (2008) 9143;
(b) S. Bagheri, M.J. Nejad, F. Pazoki, M.K. Miraki, A. Heydari, *ChemistrySelect* 4 (2019) 11930–11935;
(c) A. Garg, R. Hazarika, N. Dutta, B. Dutta, D. Sarma, *ChemistrySelect* (2021), <https://doi.org/10.1002/slct.202101347>;
(d) A. Garg, D. Sarma, A.A. Ali, *CRGSC* 3 (2020), 100013.
- [29] (a) V. Polshettiwar, R.S. Varma, *Chem. Soc. Rev.* 37 (2008) 1546;
(b) V. Polshettiwar, R.S. Varma, *Acc. Chem. Res.* 41 (2008) 629.
- [30] (a) J. Chen, S.K. Spear, J.G. Huddleston, R.D. Rogers, *Green Chem.* 7 (2005) 64;
(b) D. Kumar, V.B. Reddy, R.S. Varma, *Tetrahedron Lett.* 50 (2009) 2065–2068.
- [31] V.K. Vladimirov, R.M.A. Diego, R.R.B. Arnold, *Tetrahedron Lett.* 49 (2008) 3097.
- [32] (a) Q. Huang, M. Zheng, S. Yang, C. Kuang, C. Yu, Q. Yang, *Eur. J. Med. Chem.* 46 (2011) 5680–5687;
(b) L.S. Kallander, Q. Lu, W. Chen, T. Tomaszek, G. Yang, D. Tew, et al., *J. Med. Chem.* 48 (2005) 5644–5647.
- [33] S. Payra, A. Saha, S. Banerjee, *ChemCatChem* 10 (2018) 5468–5474.
- [34] Y. Zhao, D.G. Truhlar, *Theor. Chem. Acc.* 120 (2008) 215.
- [35] M.J. Frisch, G.W. Trucks, H.B. Schlegel, G.E. Scuseria, M.A. Robb, J.R. Cheeseman, G. Scalmani, V. Barone, G.A. Petersson, H. Nakatsuji, X. Li, M. Caricato, A. V. Marenich, et al., *Gaussian 16 (Revision A.03)*, Gaussian, Inc., Wallingford CT, 2016.
- [36] (a) M.L. Kantam, J. Yadav, S. Laha, S. Jha, *Synlett* (2009) 1791–1794;
(b) B. Sreedhar, A.S. Kumar, P.S. Reddy, *Tetrahedron Lett.* 51 (2010) 1891–1895;
(c) D. Bhuyan, M. Saikia, L. Saikia, *Catal. Commun.* 58 (2015) 158–163;
(d) F.M. Moghaddam, S.E. Ayati, S.H. Hosseini, A. Pourjavadi, *RSC Adv.* 5 (2015) 34502–34510;
(e) A.M. Munshi, M. Shi, S.P. Thomas, M. Saunders, M.A. Spackman, K.S. Iyera, N. M. Smith, *Dalton Trans.* 46 (2017) 5133–5137.